Characterization of novel spacecraft materials under high energy electron and atomic oxygen exposure

Elena A. Plis*
Georgia Tech Research Institute (GTRI), Atlanta, GA, 30318, USA; Assurance Technology Corporation, Carlisle, MA, 01741, USA

Miles T. Bengtson†
National Research Council Research Associateship Program, 3550 Aberdeen Ave., Kirtland AFB, New Mexico 87117, USA

Daniel P. Engelhart‡
University of New Mexico, Albuquerque, NM, 87131, USA

Gregory P. Badura§
Georgia Tech Research Institute (GTRI), 925 Dalney St NW, Atlanta, GA 30318

Heather M. Cowardin¶
NASA Johnson Space Center, Orbital Debris Program Office, 2101 NASA Pkwy., Houston, TX 77058, USA

Jacqueline A. Reyes‖
University of Texas at El Paso, 500 W. University Ave., El Paso, TX, 79968, USA

Ryan C. Hoffmann, Alexey Sokolovskiy, Dale C. Ferguson**
Air Force Research Laboratory, Space Vehicles Directorate, USA, Kirtland AFB, Albuquerque, NM, 87117, USA

Jainisha R. Shah and Sydney Horne, ††
Assurance Technology Corporation, Carlisle, MA, 01741, USA

Timothy R. Scott‡‡
DuPont de Nemours, Inc, Durham, NC 27703, USA

The harsh space environment imposes stringent requirements upon spacecraft materials, especially those located on exterior surfaces of space objects in low Earth orbit (LEO). As humankind moves from space exploration to space commercialization, these polymers may have to last for 15–20 years without considerable degradation of their material properties. Hence, we must understand the effects of the space environment on materials currently in use as well as on untested materials. In the presented study authors exposed several space-relevant polymers to the simulated space weather comprised by electrons and atomic oxygen irradiation. First, materials were thoroughly characterized in their pristine state to create a baseline for the ground- and space-based experiments. Next, alteration of optical, surface, and charge transport properties of the same materials were studied under space-simulated environment.

*Senior Research Engineer, Georgia Tech Research Institute (GTRI), 925 Dalney St NW, Atlanta, GA 30318; Assurance Technology Corporation, Carlisle, MA, 01741, USA

†Postdoctoral Fellow, National Research Council Research Associateship Program, 3550 Aberdeen Ave., Kirtland AFB, New Mexico 87117, USA

‡Research Professor, Department of Chemistry and Chemical Biology, University of New Mexico, 300 Terrace St NE, Albuquerque, NM, 87131.

§Research Scientist, Georgia Tech Research Institute (GTRI), 925 Dalney St NW, Atlanta, GA 30318.

¶Laboratory and In Situ Lead Orbital Debris Business Unit Manager, NASA Johnson Space Center, Orbital Debris Program Office, 2101 NASA Pkwy., Houston, TX 77058, USA

‖University of Texas at El Paso, 500 W. University Ave., El Paso, TX, 79968, USA

**Air Force Research Laboratory, Space Vehicles Directorate, USA, Kirtland AFB, Albuquerque, NM, 87117, USA

††Assurance Technology Corporation, Carlisle, MA, 01741, USA

‡‡Business Development Leader, Aerospace & Defense, DuPont de Nemours, Inc, Durham, NC 27703.

I. Introduction

As humankind's forays into space become simultaneously more commonplace and ambitious, the need for a fundamental understanding of the interactions between the harsh space environment and spacecraft materials becomes ever more important. Research has shown that the physical, chemical, and optical properties of matter change continuously as a result of exposure to solar radiation and aggressive chemical species produced in Earth's upper atmosphere. A thorough knowledge of the evolution of material properties throughout a planned mission lifetime is of primary importance when designing long-term space missions. Further, as the requirements for new space missions become more stringent and extensive, novel lightweight materials must be developed with improved long-term radiation shielding and mechanical properties for use in internal and external spacecraft systems. Newly developed materials must be thoroughly vetted before implementation. Characterization of heritage materials in the space environment is also necessary for identification and tracking of orbital debris, a crucial first step toward debris remediation [1, 2].

Ground-based simulation of the space environment is experimentally challenging because the space environment varies wildly depending on orbit, solar conditions, and many other factors [3]. Accurate space weather simulation must include several different species of radiation, charged and uncharged chemical species, and temperature fluctuations [4]. Precise material characterization is also demanding as post-irradiation measurements must be carried out in vacuum or under inert gas flow, as atmospheric gases can participate in post-irradiation material chemistry, rendering any results non-representative of a material's actual behavior on orbit. Therefore, ground testing requires thorough validation in order to develop trustworthy models of material degradation.

One major barrier to utilizing novel materials on spacecraft is the immense cost of flying to space. With exact knowledge of material properties throughout an expected mission lifetime, the best material can be chosen to ensure optimal performance for the entirety a spacecraft's mission. By developing thorough and accurate ground-based space weather simulation capabilities, the barrier to vetting new materials will be reduced considerably. A newfound freedom in material selection could very well lead to dramatic advances in design that would otherwise be unfeasible.

The the Materials International Space Station Experiment Flight Facility (MISSE-FF) at International Space Station (ISS) is the perfect test bed to generate benchmark data with which to validate the efficacy of ground-based space weather simulation experiments [5, 6]. Our ultimate goal is to fly several novel and well-understood materials on the MISSE-FF and monitor the changes in spectral reflectivity that occur as a result of exposure to different components of the low Earth orbit (LEO) environment. Energy deposition from the environment leads to chemical changes in the material that in turn alter the optical properties. The same chemical damage that manifests as changes in optical reflectance and absorptance also leads to changes in myriad physical properties such as mechanical strength, electrical conductivity, and chemical reactivity [7–10]. Correlation of the changes in each of these properties as function of radiation flux and fluence will allow us to infer a host of material properties based on one experimentally convenient measurement: color change. By flying identical test fixtures on the ram, zenith, and wake positions of the MISSE-FF and collecting spectrally resolved images of the materials throughout the mission along with concomitant measurement of the ambient space environment, we may measure the optical changes that occur in each material as a function of exposure to neutral atomic oxygen (AO), unfiltered solar ultraviolet (UV) radiation, and electrons, respectively. Correlation of the MISSE data with extensive testing of flight-duplicate (AO-, UV-, and electron-exposed) and control (pristine) samples will enable development of fundamental chemical models for material degradation.

In presented study, several spacecraft polymers were first thoroughly characterized in their pristine state to create a baseline for the ground- and space-based experiments. Next, alteration of optical, surface, and charge transport properties of the same materials were studied under space-simulated environment comprised by, separately, high-energy electron and AO exposure. The same material selection is planned to be flown during the MISSE-16 mission; however, the space experiment data as well as their comparison with the results of ground experiments is the subject of future publication.

II. Experimental Details

A. Materials

This study focuses on several visually white materials from the different classes of polymers, namely, polyimides (PIs) (Kapton®WS Glossy), Polyethyleneterephthalate or PET (Melinex®454, M021), liquid crystal polymer (Zenite®), and PI/Polyhedral Oligomeric Silsesquioxanes (POSSs, Thermalbright™N), as shown in Table 1.

Kapton®has been used for more than 50 years to protect nearly every satellite, spacecraft, and astronaut since Apollo 11. The Kapton®WS Glossy is an opaque film with high thermal stability; possible alternative for traditional PI film in

Table 1 Studied spacecraft polymers.

Material	Abbrev.	Thickness (mil)	Potential application
Kapton®WS Glossy	PI	1	Thermal control foils
Melinex®454	PET	5	Improved reflectivity of MLI
Mylar®M021	PET	10	Improved reflectivity of MLI
Zenite®	LCP	3	Flexible antennas and circuits
Thermalbright™N	POSS	0.8	AO-resistive insulation

*MLI stands for the multi-layer insulation

**Trade names and trademarks are used in this report for identification only. Their usage does not constitute an official endorsement, either expressed or implied, by the National Aeronautics and Space Administration.

MLI blankets.

PET film, more often known by its trade name Mylar, is an essential part of MLI blankets that are used on the exterior surfaces of spacecraft for the purpose of passive thermal control. These composite materials work by limiting the amount of radiative heat transfer through multiple layers of thin reflectors and spacer materials. An ideal thermal blanket reflects 100% of the incident radiation. In practice, this ideal value has not been obtainable using traditional MLI blankets. Thus, new materials, such as Melinex®454 and Mylar®M021 need to be developed for improved MLI reflectivity and durability.

LCPs present a special category of materials, which straddles the boundary between an ordinary solid and a liquid. LCPs have excellent dimensional stability (fatigue and creep resistance), as well as high dielectric strength over wide temperature range[11]. Moreover, LCPs show a high resistance to UV radiation and very good electrical insulation properties [12]. These unique properties in conjunction with light weight make LCP materials very attractive for space applications. Flexible LCP antennas and LCP-based circuits molded to available spacecraft areas could eliminate heavy metal boxes that currently house rigid circuit boards [13].

PI/Polyhedral Oligomeric Silsesquioxane (POSS) hybrid materials were proposed to increase the AO-resistivity of PI films by incorporation of the monomer POSS into the PI polymer matrix, either as a chemically bound co-polymer or an additive blended into the matrix [14]. The unique benefit of this method over traditional methods, such as coatings, is that when POSS-PI is initially exposed to AO, it forms a layer of SiOx over the surface. This passivating layer prevents further material ablation, thus lowering the overall erosion yield. Moreover, if the surface is damaged in anyway and cracks appear, the newly exposed surface will simply form another layer of SiOx. Hence, POSS-PI essentially a self-healing polymer. As PI/POSS hybrid materials have already been identified as excellent AO resistant materials, a detailed study of Thermalbright™PI's optical properties will be of great utility to the remote sensing community for the characterization of orbital debris.

Figure 1 demonstrates the photographs of studied materials in their pristine state.

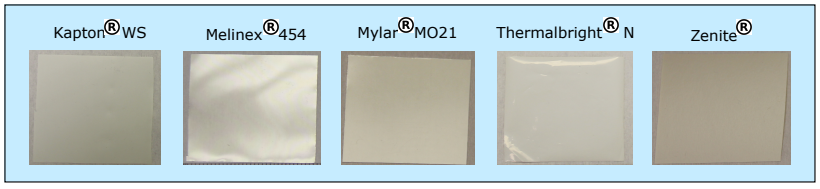

Fig. 1 Photographs of materials under study in their pristine state

B. Irradiation procedure

High energy electron irradiation was performed with high energy (100 keV) mono-energetic electron radiation from a Kimball Physics EG8105-UD electron flood gun in the Spacecraft Charging and Instrument Calibration Laboratory (SCICL) at Kirtland Air Force Base in New Mexico, USA [15]. Samples were mounted over a reflective aluminum surface of the same area, then samples were adhered to a carousel that rotated through the hot spot of the electron beam to ensure uniform irradiation. Prior to the radiation exposure, the 100 keV electron beam was characterized via a

Faraday cup (FC) housed in the center of the carousel. The relative geometry of the hot spot of the electron beam, the FC, and the sample positions on the rotating carousel are shown in Figure 2. More details of the electron irradiation procedure are reported elsewhere [16]. Materials were irradiated to the maximum fluence of 4 x 10^{13} electrons/cm^2, which corresponds to approximately one year of equivalent LEO exposure. AO exposure was performed using the FAST source at the Physical Sciences Inc, as shown in Figure 3 in according to ASTM-E2089-15. The effective peak atomic oxygen fluence during the exposure was 3.1 x 10^{20} O/cm^2. The 8 km/s O-atom beam was generated in high vacuum chamber with pulsed laser discharge. AO exposure fluence was determined using the reference Kapton®H and the published erosion rate for Kapton®H by 5 eV AO, 3 x 10^{24} cm^3/AO. During the exposure, temperature was controlled (25C) across the 11.4 cm x 11.4 cm sample holder to accommodate simultaneous and uniform exposure of materials.

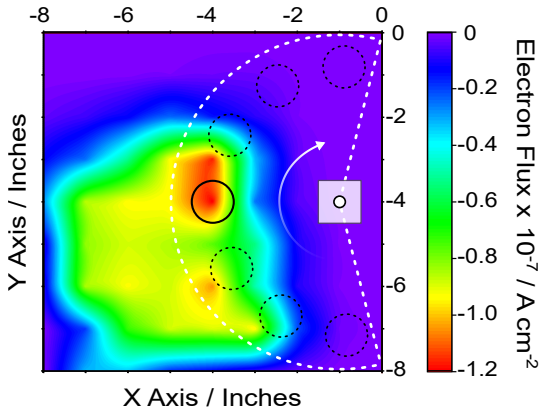

Fig. 2 Flux map for the 100 keV electron beam. Relative positions of the sample carousel (white dashed line), the FC (white square), and the mounted samples (black dashed circles) are shown. A sample remains in the hot spot of the beam (solid black circle) for a total of 60 seconds before the carousel is rotated clockwise (direction indicated by the white arrow).

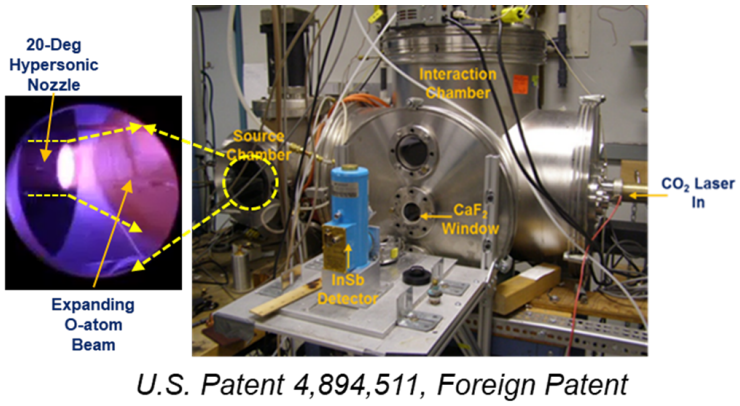

Fig. 3 FAST source utilized for the AO exposure of materials. Image credit: Physical Sciences Inc.

C. Materials characterization

1. Surface properties

Surface morphology and roughness of studied materials was examined using Bruker Dimension ICON atomic force microscopy (AFM) allowing measurement of surface roughness up to 5 μm on areas as large as 200 μm x 200 μm.

2. Optical properties

Transmittance and reflectance of pristine materials were characterized using Perkin-Elmer UV/Vis spectrometer within 200 – 2500 nm spectral range. In addition, Fourier-Transform Infrared (FTIR) spectroscopy measurements are utilized to identify the vibrational bands of different chemical moieties of pristine and irradiated materials. The usual practice of plotting transmission (in %), as a function of wavenumber (in 1/cm), has been followed. The minima or dips in the transmission spectra refer to absorption maxima corresponding to characteristic molecules and groups. The direct hemispherical reflectance (DHR) measurements of pristine and irradiated films will be also measured during the irradiation procedure in according to the optical data acquisition procedure reported elsewhere [17]. Finally, the Hemispherical Conical Reflectance Factor (HCRF), the laboratory approximation of true Bidirectional Reflectance Distribution Function (BRDF) measurements, of pristine samples with fixed viewing angles (0°, 30°, 60°, -30°, and -60°) and variable illumination angles (0° - 70° degrees range, exact values of illumination angles are specified separately for each measurement), was evaluated in the principal plane of illumination. The samples were illuminated with a collimated 50 Watt tungsten halogen that approximated a blackbody source over the range of 350-2500 nm. An Analytical Spectral Devices Spectrometer was used to collect radiance measurements over this spectral range.

3. Charge transport properties

To assess the charge transport properties of pristine and irradiated materials the surface potential decay (SPD) method was utilized [18]. In short, the SPD method uses a low energy electron gun to dust electrons onto the surface of an insulating material with a grounded backing. Next, the charging beam is extinguished and the resultant surface potential is then measured as a function of time using a non-contact electric field probe (TREK model 370). As the electrons are transported through the material, the surface potential will decay towards zero. The rate of this decay is directly related to the electrical conductivity of the material.

4. Mass loss

Mass loss of AO-exposed materials was measured with 10 microgram accuracy using the microgram balance. Prior weight measurements, all samples were stored in the vacuum chamber for 24 hours to remove water. They were then removed and weighed over time to monitor water absorption and allow for the dry mass to be calculated. Next, AO-erosion rate was estimated.

III. Results

A. Electron exposure

In according to [19], mean annual electron flux (>100 keV, electrons, orbit averaged) experienced by the International Space Station (ISS) is 10^{13} electrons/cm^2/second. The maximum electron fluence the materials under investigation were exposed to is 2.2 x 10^{14} electrons/cm^2, which corresponds to approximately ten years at 600-800 km (LEO) orbit, delivered during 5.5 hours. Visual inspection did not reveal significant discoloration of the irradiated materials after irradiation with maximum electron fluence.

Table 2 summarizes the surface roughness of pristine and electron-irradiated samples accessed by AFM. Average surface roughness (R_a) values are average of several 5μm x 5μm scans taken at different parts of the pristine and electron-irradiated samples. Figure 4 shows representative AFM scans for each studied sample. Surface roughness of all irradiated materials, except Zenite®, improved in the range of 4.3 - 43.6 nm.

Table 2 Surface roughness of pristine and electron-irradiated polymer samples

Material	Pristine (R_a, nm)	Irradiated (R_a, nm)
Kapton®WS Glossy	72.3	28.7
Zenite®	14.9	22.6
Melinex®454	8.2	4.9
Mylar®M021	7.8	3.5
Thermalbright®N	52.5	18.1

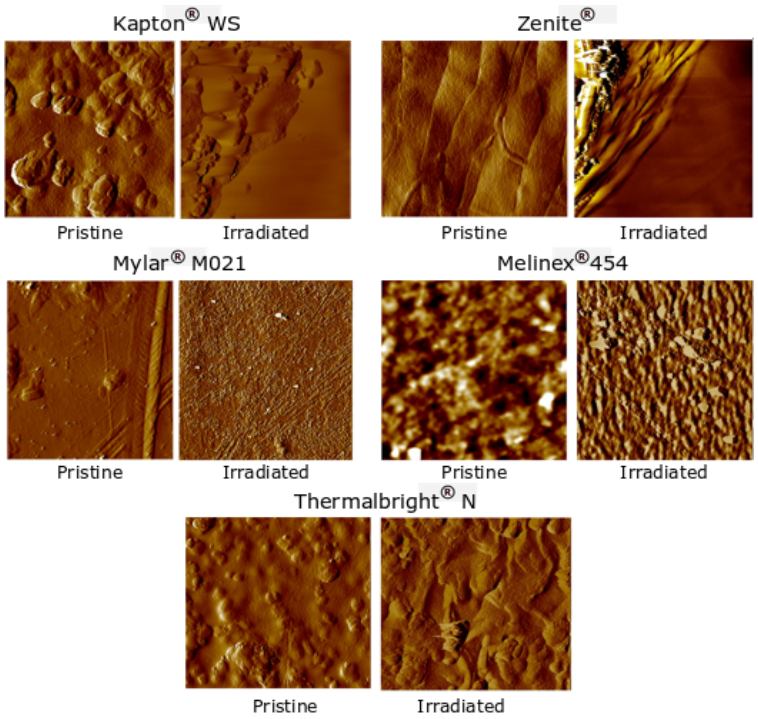

Fig. 4 Representative 5μm x 5μm AFM scans of pristine and electron-irradiated materials.

Values of volume resistivities of pristine and electron-irradiated with maximum fluence materials measured by the SPD method are summarized in Table 3. Charge transport properties of irradiated materials were affected by the electron irradiation; Kapton®WS demonstrated one order of magnitude reduction of its resistivity. Resistivity of Melinex®454 was also reduced but only by factor of 1.3. Another PET material, Mylar®M021, became essentially an insulator, and resistivity of Zenite®as well as Thermalbright®N materials was increased by an order of magnitude.

Table 3 Volume resistivities of studied materials in their pristine and electron-irradiated states measured by the SPD method.

Material	Pristine (Ω·cm)	Irradiated (Ω·cm)
Kapton®WS Glossy	$4.5 \cdot 10^{19}$	$6.9 \cdot 10^{18}$
Zenite®	$1.2 \cdot 10^{19}$	$7.9 \cdot 10^{20}$
Melinex®454	$9.6 \cdot 10^{18}$	$7.5 \cdot 10^{18}$
Mylar®M021	$4.3 \cdot 10^{18}$	$2.0 \cdot 10^{22}$
Thermalbright®N	$1.6 \cdot 10^{19}$	$1.2 \cdot 10^{22}$

Figure 5 displays the absolute reflectance spectra of pristine and irradiated with high-energy electrons polymer materials. Irradiation with maximum electron fluence degraded the reflectance of each material in 400 - 800 nm range except Thermalbright®N. Degree of the change depends on the material, with maximum degradation demonstrated by the Melinex®454 at 350-420 nm range.

Figure 6 demonstrates the FTIR spectra of pristine and electron-irradiated materials in 400 - 1800 1/cm range. It should be noted that no new peaks are generated after electron exposure, suggesting that no new chemical moieties are formed.

Figure 7 demonstrates the results of HCRF measurements of for pristine and irradiated materials performed at fixed viewing angle (30°) and variable illumination angles. It should be noted that all studied materials showed a significant reduction in specular reflection – both in terms of the peak specular signature and the width of the specular lobe.

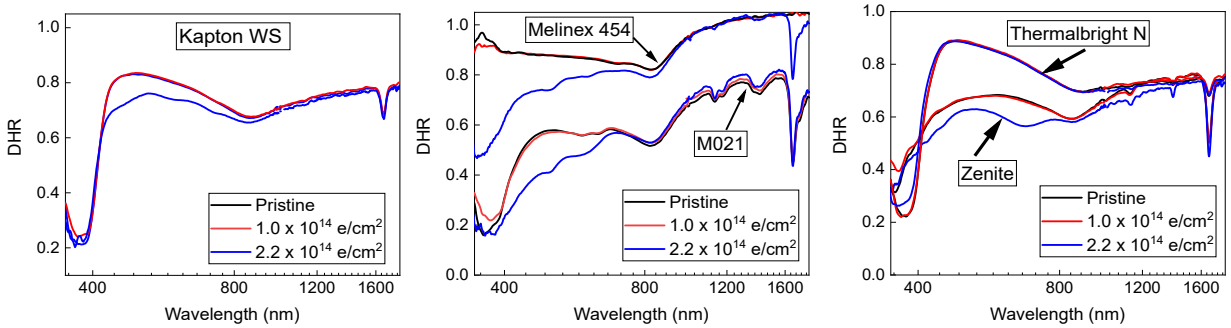

Fig. 5 DHR values of pristine and irradiated with high-energy electrons materials: (left panel) Kapton®WS, (central panel) PET samples, Melinex®454 and Mylar®M021, and (right panel) PI/POSS material, Thermalbright®N and liquid crystal polymer, Zenite®

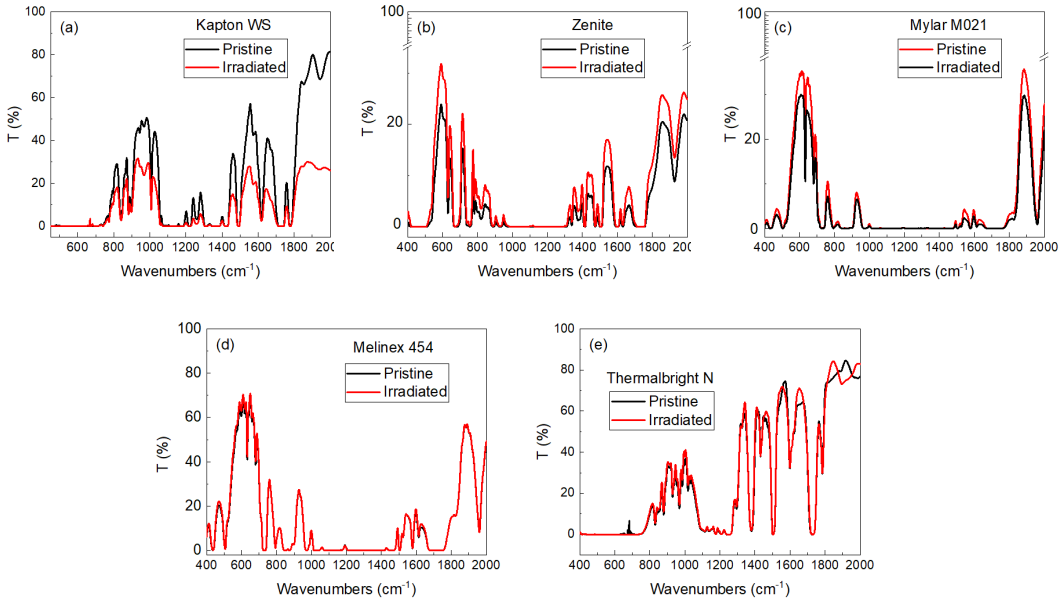

Fig. 6 FTIR spectra of pristine (black curves) and irradiated (red curves) materials showing transmittance as a function of wavenumber for the range (400 - 2000) 1/cm. (a) Kapton®WS, (b) Zenite®, (c) Mylar®M021, (d) Melinex®454, and (d) Thermalbright®N.

B. AO exposure

Exposure of polymer materials to AO at 8 km/s is sufficient to break the polymer bonds and induce oxidative decomposition, resulting in substantial erosion of polymer surfaces which manifests itself as the mass loss, thinning, and texture roughening. The rough texture results in degradation of optical properties, as illustrated by Fig. 8. Post-irradiated PET samples (Mylar®M021 and Melinex®454) as well as LCP sample (Zenite®) show hazy white surface which is result of O-atom erosion leading to the microscopic roughness of these samples. Kapton®WS and Thermalbright®N materials retained their pristine-like visual appearance suggesting the less AO-damaged, if any, surface.

Mass loss and the relative (to Kapton®H) erosion rate were evaluated and are presented in Table 4. The erosion rates for the samples ranged from .17 to 1.70, relative to the erosion rate of the Kapton®H witness samples.

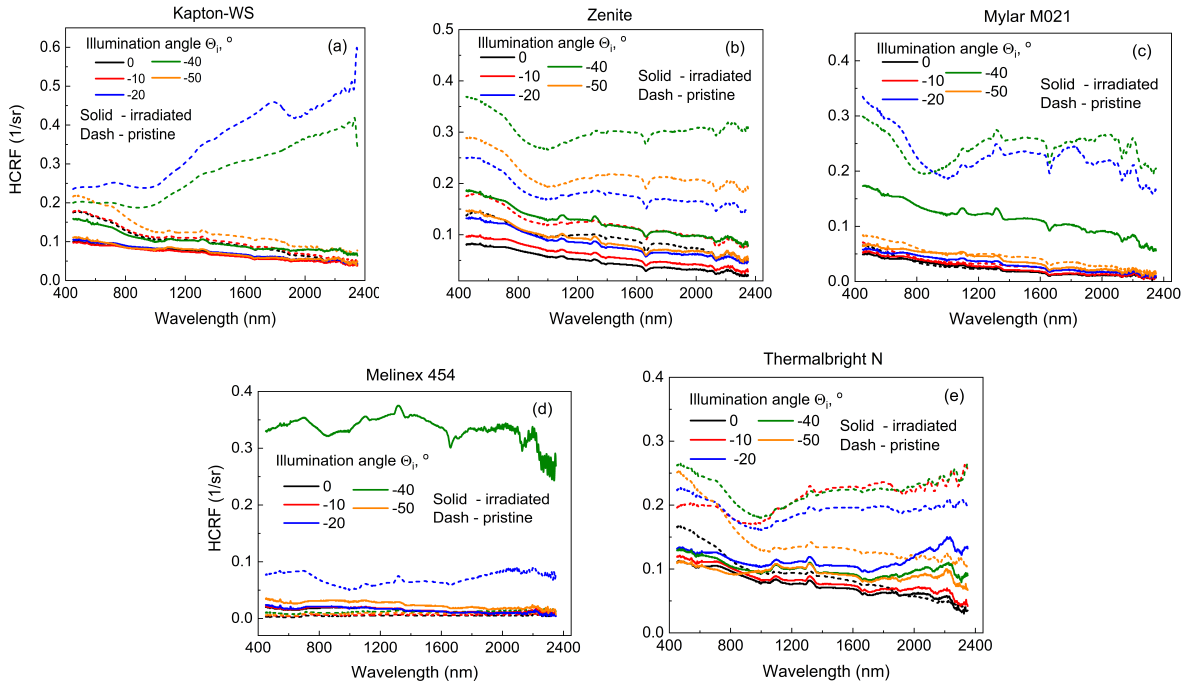

Fig. 7 HCRF measured for pristine and irradiated with maximum electron fluence (a) Kapton®WS, (b) Zenite®, (c) Mylar®M021, (d) Melinex®454, and (d) Thermalbright®N materials with fixed viewing angle (30°) and variable illumination angles.

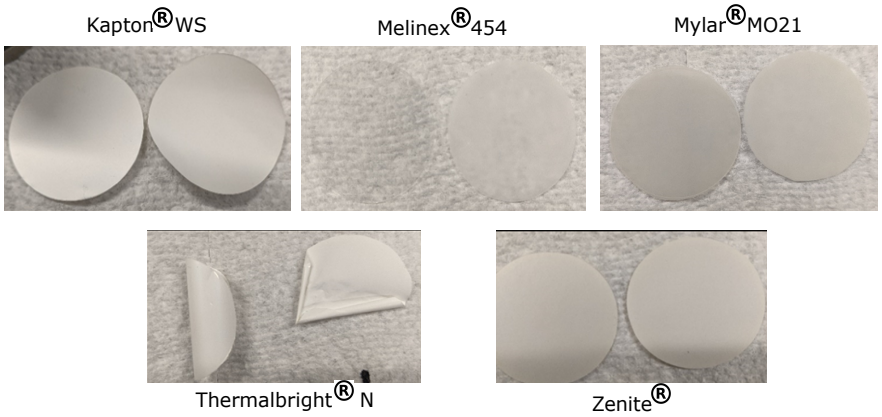

Fig. 8 Photographs of pristine (left sample on each picture) and exposed to AO (right sample on each picture) materials: (top left panel) Kapton®WS, (top central panel) Melinex®454, (top right panel) Mylar®M021, and (right panel) PI/POSS material, (bottom left panel) Thermalbright®N, and (bottom right panel) liquid crystal polymer, Zenite®

.

IV. Discussion

A. PI (Kapton®WS)

Visual inspection of post electron-irradiated material revealed no visible color change. Similarly, no surface color degradation after AO-exposure was observed. Due to the small mass of impinging electrons, no significant roughening of surface was expected after electron irradiation. However, electron-irradiated material appeared smoother compared to its pristine state (R_a of 28.7 nm and 72.3 nm, respectively). Similarly, Mishra et al. [20] reported that irradiation of

Table 4 Mass loss and the relative (to Kapton®H) erosion rate of AO-irradiated materials.

Material	Mass loss (mg)	Erosion rate
Kapton®WS Glossy	1.71	0.22
Zenite®	2.12	0.47
Melinex®454	8.01	1.64
Mylar®M021	7.89	1.70
Thermalbright™N	1.23	0.17

PI with high energy (2 MeV) electrons resulted in reduced mean surface roughness of irradiated material. Increased level of cross-linking in irradiated PI [8] may be responsible for the overall surface flattening.

Alike other PI films [19], conductivity of Kapton®WS increased after electron irradiation. The observed bulk conductivity increase in irradiated PI may be attributed to the radiation-induced generation of electron hopping sites and the formation of extended pi-bonded chemical structures which are not present in the pristine material.

Overall reflectance of Kapton®WS material reduces with high energy electrons irradiation in 380 - 860 nm range and stays unchanged afterwards. Sharp absorption edge around 380 nm demonstrated by the material correlates with its visibly white appearance. The nearly zero reflectance in shorter wavelength region (below 380 nm) exhibited by both pristine and damaged PIs is associated with absorption due to the π - π^* transitions in the aromatic groups [21]. Absorption feature at 1650 nm may be attributed to CH_3 in the first overtone [22]

The FTIR spectrum of irradiated PI did not reveal any additional bands; however, increase of absorption intensity of overall spectrum was observed. Since every minima position in transmission FTIR spectrum is fundamental to molecular bonding structure or functional group existing in the infrared active material, no new functional groups as well as no change in bond strength or bond angle was observed after irradiation. Variation in intensity correlates to the proportion of that functional group present in the material, so increased overall absorption intensity of irradiated spectrum associates with the increased degree of radiation-induced cross linking. As was reported earlier [8], increased degree of crosslinking in electron-irradiated PI is likely due to the formation of new inter-chain C–N bonds.

HCRF measurements of irradiated material demonstrated significant reduction of signal intensity, especially at -20° and -40° illumination angles (the viewing angle was fixed and corresponds to 30°).

B. LCP (Zenite®)

No electron-induced optical degradation was observed; AO-exposure caused the hazy white finish of the treated material, attributed to the surface morphology modification due to the O-erosion. Surface roughness of electron-irradiated Zenite®material was increased compared to its pristine state (22.6 nm and 14.9 nm, respectively). Electron bombardment induced the increased electrical resistivity of the Zenite®. Reflectance values of the irradiated Zenite®were overall decreased in (300 - 1600) nm region. FTIR spectrum demonstrated significantly increased overall transmission in (400 - 2000) 1/cm region suggesting, along with the increased surface roughness, increased disorder of polymer chains in the LCP structure. HCRF measurements of irradiated material demonstrated significant reduction of signal intensity at all illumination angles (the viewing angle is fixed and corresponds to 30°).

C. PET (Melinex®454, Mylar®M021)

Whereas electron bombardment produced no visible color change of both PET samples, AO-exposure significantly degraded surface quality of of Mylar®M021 and Melinex®454, resulting in their hazy white appearance. This is attributed to the formation of so-called "rag" structure caused by the O-erosion of the polymers [23]. Surface roughness of both PET materials was reduced after electron irradiation. Earlier, Chinaglia et al. [24] and Lee et al. [25] demonstrated that after low-energy (0-20 keV) electron irradiation the PET material acquires the enhanced surface smoothness. Similar observations were reported by Mishra et al [20] after irradiation of PET samples with high energy (2 MeV) electrons.

It is interesting to note that resistivity of the electron-irradiated PET samples either increased (Mylar®M021) or did not change significantly (Melinex®454). Similar phenomenon was observed by Chaudhary et al. [26] and Oproiu et al. [27]. They attributed this phenomenon to the increased crosslinking of the PET chains due to the electron irradiation, which in turn may obstruct the charge carrier from hopping from one chain to another chain resulting in decrease of

electrical conductivity.

Melinex®454 demonstrated the drastic degradation of electron-irradiated material reflectance in the region below 835 nm. The same trend, whereas not so prominent, was demonstrated by the irradiated Mylar®M021 sample. Another important feature of the Melinex®454 material caused by irradiation is the appearance of intense absorption band at 1650 nm. The Mylar®M021, irradiated to the maximum fluence, revealed a slight (3%) increase of the reflectance beyond 850 nm. Finally, additional radiation -induced absorption features appeared in both materials; at 500 nm and 600 nm for Melinex®454, and at 500 nm for Mylar®M021.

FTIR transmission spectrum of electron-irradiated Melinex®454 did not show any changes compared to the prsitine material. The irradiated FTIR spectrum of Mylar®M021 demonstrated slightly increased overall transmission, with increased intensity of absorption at 631 1/cm, characteristic for the methylene group [28].

HCRF measurements of irradiated material demonstrated reduction of signal intensity at all illumination angles for Mylar®M021 sample. Similar trend was observed for Melinex®454, except the HCRF signal at -40° illumination angle, which revealed approximately factor of 10 higher signal. The viewing angle was fixed and corresponds to 30°.

D. PI/POSS (Thermalbright®N)

The Thermalbright®N material demonstrated no visible degradation of optical surface quality after electron irradiation and a pristine-like appearance after the AO-exposure. The enhanced durability of PI/POSS under AO exposure is a result of a silica passivation layer formation on top of the degraded organic material (PI) during the AO-bombardment [29]. This silica layer protects the underlying polymer from further degradation resulting in the lowest erosion rate of the Thermalbright®N material among the studied samples. Electron irradiation enhanced smoothness of the material; average surface roughness was 52.5 nm for the pristine and 18.1 nm for the irradiated films, respectively.

While Thermalbright®N is referred as a white polyimide, unlike polyimides from the Kapton ®family it became significantly more resistive after electron irradiation, with volume resistivity of irradiated material being a factor of 1000 higher compared to the pristine one.

DHR spectrum of the electron-irradiated POSS material showed no change of reflectance with irradiation to the maximum electron fluence. Comparison of FTIR spectra of pristine and electron-irradiated Thermalbright®N revealed radiation-induced increased absorption in (670 - 700) 1/cm region and at 1900 1/cm. HCRF measurements of irradiated material demonstrated the overall reduction of signal intensity at all illumination angles .

V. Conclusions

Thorough physical and chemical characterization of novel and heritage spacecraft materials during the simulated space weather experiments is important for establishment of correlation factors between true space-exposure and accelerated space weather experiments at ground facilities as well as enabling accurate prediction of on-orbit material performance based on laboratory-based testing. This work focuses on characterization of material properties of selected spacecraft materials under independent LEO-simulated electron irradiation and AO exposure.

VI. Acknowledgements

Authors gratefully acknowledge Physical Sciences, Inc., especially Drs. Daniel M. Hewett and David B. Oakes, for conducting AO-exposure experiments. Authors also would like to thank DuPont de Nemours, Inc, for providing polyimide materials for this research. This work was partially supported by Air Force Office of Scientific Research, Remote Sensing and Imaging Physics Portfolio (Dr. Michael Yakes) Grant 20RVCOR024 and Georgia Tech Research Institute Independent Research and Development (IRAD) program.

References

[1] McKnight, D., Witner, R., Letizia, F., Lemmens, S., Anselmo, L., Pardini, C., Rossi, A., Kunstadter, C., Kawamoto, S., Aslanov, V., Perez, J.-C. D., Ruch, V., Lewis, H., Nicolls, M., Jing, L., Dan, S., Dongfang, W., Barranov, A., and Grishko, D., "Identifying the 50 statistically-most-concerning derelict objects in LEO," *Acta Astronautica*, Vol. 181, 2021, pp. 282–291.

[2] Reyes, J. A., and Cowardin, H. M., "Spectral characterization of spacecraft materials used in hypervelocity impact testing," *Algorithms, Technologies, and Applications for Multispectral and Hyperspectral Imaging XXVII*, Vol. 11727, International Society for Optics and Photonics, 2021, p. 117271G.

[3] Gordo, P., Frederico, T., Melício, R., Duzellier, S., and Amorim, A., "System for space materials evaluation in LEO environment," *Advances in Space Research*, Vol. 66, No. 2, 2020, pp. 307–320.

[4] Lu, Y., Shao, Q., Yue, H., and Yang, F., "A review of the space environment effects on spacecraft in different orbits," *IEEE Access*, Vol. 7, 2019, pp. 93473–93488.

[5] deGroh, K. K., Dever, J. A., Jaworske, D. A., Miller, S. K., Sechkar, E. A., Panko, S. R., et al., "NASA Glenn research center's materials international space station experiments (MISSE 1-7)," 2008.

[6] de Groh, K. K., and Banks, B. A., "Atomic Oxygen Interactions and the Design of MISSE-9 and MISSE-10 Experiments," 2018.

[7] Plis, E., Engelhart, D. P., Barton, D., Cooper, R., Ferguson, D., and Hoffmann, R., "Degradation of polyimide under exposure to 90 keV electrons," *physica status solidi (b)*, Vol. 254, No. 7, 2017, p. 1600819.

[8] Rahnamoun, A., Engelhart, D. P., Humagain, S., Koerner, H., Plis, E., Kennedy, W. J., Cooper, R., Greenbaum, S. G., Hoffmann, R., and van Duin, A. C., "Chemical dynamics characteristics of Kapton polyimide damaged by electron beam irradiation," *Polymer*, Vol. 176, 2019, pp. 135–145.

[9] Alegaonkar, P., Bhoraskar, V., Balaya, P., and Goyal, P., "Dielectric properties of 1 MeV electron-irradiated polyimide," *Applied physics letters*, Vol. 80, No. 4, 2002, pp. 640–642.

[10] Mishra, R., Tripathy, S., Dwivedi, K., Khathing, D., Ghosh, S., Müller, M., and Fink, D., "Spectroscopic and thermal studies of electron irradiated polyimide," *Radiation measurements*, Vol. 36, No. 1-6, 2003, pp. 621–624.

[11] White, T. J., and Broer, D. J., "Programmable and adaptive mechanics with liquid crystal polymer networks and elastomers," *Nature materials*, Vol. 14, No. 11, 2015, pp. 1087–1098.

[12] Campo, E. A., *Complete Part Design Handbook*, Hanser Germany, 2006.

[13] Gupta, S., "Application of Liquid Crystals in Space Activities," *Frontiers of Polymer Research*, Springer, 1991, pp. 189–193.

[14] Brunsvold, A. L., Minton, T. K., Gouzman, I., Grossman, E., and Gonzalez, R., "An investigation of the resistance of polyhedral oligomeric silsesquioxane polyimide to atomic-oxygen attack," *High Performance Polymers*, Vol. 16, No. 2, 2004, pp. 303–318.

[15] Cooper, R., and Hoffman, R., "Jumbo space environment simulation and spacecraft charging chamber characterization," Tech. rep., Air Force Research Laboratory, Space Vehicles Directorate Kirtland AFB . . . , 2015.

[16] Engelhart, D. P., Plis, E., Humagain, S., Greenbaum, S., Ferguson, D., Cooper, R., and Hoffmann, R., "Chemical and electrical dynamics of polyimide film damaged by electron radiation," *IEEE Transactions on Plasma Science*, Vol. 45, No. 9, 2017, pp. 2573–2577.

[17] Bengtson, M., Maxwell, J., Hoffmann, R., Cooper, R., Schieffer, S., Ferguson, D., Johnston, W. R., Cowardin, H., Plis, E., and Engelhart, D., "Optical characterization of commonly used thermal control paints in a simulated GEO environment," *The Advanced Maui Optical and Space Surveillance Technologies Conference*, 2018, p. 33.

[18] Frederickson, A. R., and Dennison, J., "Measurement of conductivity and charge storage in insulators related to spacecraft charging," *IEEE Transactions on Nuclear Science*, Vol. 50, No. 6, 2003, pp. 2284–2291.

[19] Plis, E. A., Engelhart, D. P., Cooper, R., Johnston, W. R., Ferguson, D., and Hoffmann, R., "Review of radiation-induced effects in polyimide," *Applied Sciences*, Vol. 9, No. 10, 2019, p. 1999.

[20] Mishra, R., Tripathy, S., Dwivedi, K., Khathing, D., Ghosh, S., Müller, M., and Fink, D., "Modification in etching characteristics and surface topography of some electron irradiated polymers," *Radiation measurements*, Vol. 34, No. 1-6, 2001, pp. 95–98.

[21] Ishida, H., Wellinghoff, S. T., Baer, E., and Koenig, J. L., "Spectroscopic studies of poly [N, N'-bis (phenoxyphenyl) pyromellitimide]. 1. Structures of the polyimide and three model compounds," *Macromolecules*, Vol. 13, No. 4, 1980, pp. 826–834.

[22] Burke, M., Dawson, C., Allen, C. S., Brum, J., Roberts, J., and Krekeler, M. P., "Reflective spectroscopy investigations of clothing items to support law enforcement, search and rescue, and war crime investigations," *Forensic science international*, Vol. 304, 2019, p. 109945.

[23] Tennyson, R., "Atomic oxygen effects on space inflatable materials," *Progress in Astronautics and Aeronautics.*, Vol. 191, 2001, pp. 281–302.

[24] Chinaglia, D., Constantino, C., Aroca, R., and Oliveira Jr, O., "Surface modifications on Teflon FEP and Mylar C induced by a low energy electron beam: A Raman and FTIR spectroscopic study," *Molecular Crystals and Liquid Crystals*, Vol. 374, No. 1, 2002, pp. 577–582.

[25] Lee, E., Lewis, M., Blau, P., and Mansur, L., "Improved surface properties of polymer materials by multiple ion beam treatment," *Journal of Materials Research*, Vol. 6, No. 3, 1991, pp. 610–628.

[26] Chaudhary, N., Koiry, S., Singh, A., Tillu, A., Jha, P., Samanta, S., Debnath, A., Aswal, D., Mondal, R., Acharya, S., et al., "Electron beam induced modifications in flexible biaxially oriented polyethylene terephthalate sheets: Improved mechanical and electrical properties," *Materials Chemistry and Physics*, Vol. 189, 2017, pp. 237–244.

[27] Oproiu, C., Martin, D., Toma, M., Marghitu, S., and Jianu, A., "Transitory and permanent effects of electron beam irradiation on insulating materials," *Nuclear Instruments and Methods in Physics Research Section B: Beam Interactions with Materials and Atoms*, Vol. 166, 2000, pp. 669–675.

[28] Dworecki, K., Hasegawa, T., Sudlitz, K., and Wąsik, S., "Modification of electrical properties of polymer membranes by ion implantation," *Nuclear Instruments and Methods in Physics Research Section B: Beam Interactions with Materials and Atoms*, Vol. 166, 2000, pp. 646–649.

[29] Minton, T. K., Wright, M. E., Tomczak, S. J., Marquez, S. A., Shen, L., Brunsvold, A. L., Cooper, R., Zhang, J., Vij, V., Guenthner, A. J., et al., "Atomic oxygen effects on POSS polyimides in low earth orbit," *ACS applied materials & interfaces*, Vol. 4, No. 2, 2012, pp. 492–502.